Locally Corrected Nyström Discretization for Impressed Current Cathodic Protection Systems

John C. Young [1], Robert A. Pfeiffer [1], Robert J. Adams [1], and Stephen D. Gedney [2]

[1] Department of Electrical and Computer Engineering
University of Kentucky, Lexington, KY 40506, USA
john.c.young@uky.edu, robert.pfeiffer@uky.edu, robert.adams@uky.edu

[2] Department of Electrical and Computer Engineering
University of Colorado-Denver, Denver, CO 80204, USA
stephen.gedney@ucdenver.edu

Abstract — A high-order locally corrected Nyström discretization for analyzing impressed current cathodic protection systems is presented. Non-linear polarization curves are incorporated using a Newton-Raphson scheme. A Schur complement scheme is introduced to handle large domains with small electrodes. The methods are characterized in terms of error convergence and computation time by comparing to the analytic solution for a sphere and hemisphere.

Index Terms — Impressed current cathodic protection systems, integral equations, locally corrected Nyström method.

I. INTRODUCTION

Hull corrosion of marine vessels has been an area of much interest since vessels began to be constructed using metal. Various methods are used to mitigate hull corrosion including painting the hull with an insulating material and using cathodic protection systems. Cathodic protection systems are primarily classified as either sacrificial or impressed current. In a sacrificial system, a more easily corroded metal is used to inject electrons into the electrolyte, whereas in an impressed current system electrons are injected directly using a battery or generator. Cathodic protection system electrodes often exhibit non-linear behavior which can be approximately modeled using polarization curves.

In this paper, an overview of the integral formulation [1-6] for the analysis of an impressed current cathodic protection (ICCP) system is presented. The equation is discretized using the arbitrary-order locally corrected Nyström (LCN) method [7-9]. The Newton-Raphson method is used to handle problems with non-linear polarization curves. A Schur complement-based method is discussed to reduce the computational complexity of the Newton-Raphson iteration when the boundary conditions are mostly constant. Validation and convergence of the method is investigated using a sphere with non-constant boundary conditions.

II. THEORY

A. Formulation

Consider a region V bound by a surface S with inward surface normal $\hat{\mathbf{n}}_i$. The region may represent either an internal or an external region, and, if the region is external, part of S recedes to infinity. Furthermore, let the region be filled with an electrolyte with conductivity σ. Green's second identity relates the electric potential Φ in the electrolyte to the boundary potential Φ and its normal derivative $\hat{\mathbf{n}}_i \cdot \nabla\Phi$ as:

$$\Phi(\mathbf{r}) - \oint_S \Phi' \nabla' G \cdot \hat{\mathbf{n}}_i' ds' - \Phi^{\infty} + \oint_S G \nabla' \Phi' \cdot \hat{\mathbf{n}}_i' ds' = 0, \quad \mathbf{r} \in V \tag{1}$$

where the additional unknown Φ^{∞} is only included for an external problem. The kernel is the static, homogeneous Green's function:

$$G(\mathbf{r}, \mathbf{r}') = \frac{1}{4\pi |\mathbf{r} - \mathbf{r}'|}. \tag{2}$$

For both the interior and exterior problems, a meaningful solution exists only if the total flux over the boundary S is zero [10]:

$$\oint_S \nabla\Phi \cdot \hat{\mathbf{n}}_i dS = 0. \tag{3}$$

Furthermore, for the linear interior Neumann problem [10], the additional constraint:

$$\oint_S \Phi dS = C, \tag{4}$$

with constant C (usually zero) is applied. Enforcement of (1) on S produces the integral equation:

Submitted On: September 28, 2018
Accepted On: October 3, 2018

$$\begin{aligned}\frac{1}{2}\Phi(\mathbf{r}) - \text{P.V.}\oint_S \Phi'\nabla' G(\mathbf{r},\mathbf{r}')\cdot\hat{\mathbf{n}}_i' ds' - \Phi^\infty \\ + \oint_S G\nabla'\Phi'\cdot\hat{\mathbf{n}}_i' ds' = 0, \quad \mathbf{r}\in S\end{aligned}. \tag{5}$$

The hull surface may be split into three parts: an insulating part S^i on which $\nabla'\Phi'\cdot\hat{\mathbf{n}}_i' = 0$, electrodes S^p on which the potential Φ is known, and electrodes S^f on which the normal derivative (flux) is known $\nabla'\Phi'\cdot\hat{\mathbf{n}}_i'$. Often electrodes S^f are polarized and are specified using a polarization curve *P* such that,

$$\hat{\mathbf{n}}_i\cdot\nabla\Phi = P(\Phi). \tag{6}$$

B. Locally corrected Nyström discretization

The integral Equation (5) with the conditions (as necessary) (3) and (4) is discretized using an arbitrary-order locally corrected Nyström (LCN) method where the surface is meshed with either triangle or quadrilateral elements of arbitrary order. As an example, the discretization of (3) and (5) for the exterior Neumann problem with polarized electrodes is:

$$\begin{aligned}\left[H^e\right]\begin{bmatrix}\Phi^f\\ \Phi^i\\ \Phi^\infty\end{bmatrix} &= \begin{bmatrix}H^{ff} & H^{fi} & -1\\ H^{if} & H^{ii} & -1\\ 0 & 0 & 0\end{bmatrix}\begin{bmatrix}\Phi^f\\ \Phi^i\\ \Phi^\infty\end{bmatrix} \\ &= \begin{bmatrix}G^{ff} & G^{fi} & 0\\ G^{if} & G^{ii} & 0\\ S^f & S^i & 0\end{bmatrix}\begin{bmatrix}P(\Phi^f)\\ 0\\ 0\end{bmatrix} \\ &= \left[G^e\right]\begin{bmatrix}P(\Phi^f)\\ 0\\ 0\end{bmatrix}\end{aligned}, \tag{7}$$

where the matrix definitions are determined by comparing (7) to (3) and (5). Note that the additional zero column in the G^e matrix is added so that H^e and G^e are of the same dimensions. Also, the S^x entries are related to the differential surface areas of the elements at the test points and are used to enforce (3).

C. Newton-Raphson method

For a non-constant polarization curve $P(\Phi)$, the Newton-Raphson method [3] is applied with the iterative update $\left[\Phi^{k+1}\right] = \left[\Phi^k\right] + \left[\delta\Phi^k\right]$ such that,

$$\left[\delta\Phi^k\right] = -\left[J\left(\Phi^k\right)\right]^{-1}\left[P\left(\Phi^{f,k}\right)\right], \tag{8}$$

where the Jacobian matrix $\left[J\right]$ at iteration *k* is:

$$\left[J\right] = \left[\frac{\partial P}{\partial\Phi^k}\right] = \left[G^e\right]\cdot\text{diag}\left(\begin{bmatrix}P'\left(\Phi^{f,k}\right)\\ 0\\ 1\end{bmatrix}\right) - \left[H^e\right]. \tag{9}$$

For large problems in which the electrodes only cover a small portion of the surface, the Schur complement can be applied to avoid factoring a full Jacobia n matrix at each iteration. A partitioning of the Jacobian matrix amenable to the Schur complement is:

$$\left[J\right] = \begin{bmatrix}G^{nc,nc}\cdot\text{diag}\left(P'\left(\Phi^{nc}\right)\right) - H^{nc,nc} & -H^{nc,co}\\ G^{co,nc}\cdot\text{diag}\left(P'\left(\Phi^{nc}\right)\right) - H^{co,nc} & -H^{co,co}\end{bmatrix} \tag{10}$$

where the superscripts *nc* and *co* indicate those portions of the matrix corresponding to non-constant and constant boundary conditions, respectively. Before the Newton-Raphson iteration begins, the matrix $H^{co,co}$ is pre-factored and stored. Then, at each Newton-Raphson step, a matrix is only factored that has the dimensions of the degrees-of-freedom associated with the electrodes having non-constant polarization curves. The above Schur complement form is also amenable for use in fast-direct solvers.

D. Image plane theory

In the event that one side of the electrolyte is completely bounded by a planar, insulating surface, then image theory may be applied to reduce the computational burden. For external problems, the insulating, planar boundary is often unbounded such as when the electrolyte fills a half-space that is bounded above by an electrolyte-air interface. In this case, the use of image theory greatly reduces the modeling burden and improves accuracy. Otherwise, the half-space must be truncated and placed inside a finite box for computation, which introduces truncation error into the solution. In addition, note that using a truncated box model changes an exterior problem into an interior one.

When image theory is applied, the planar, insulating surface is not meshed and no degrees-of-freedom are assigned to it. Instead an image Green's function,

$$G_{\text{im}}(\mathbf{r},\mathbf{r}') = G(\mathbf{r},\mathbf{r}') + G(\mathbf{r},\mathbf{r}'_{\text{im}}), \tag{11}$$

is used in (1) and (5) in place of G. Here, $\mathbf{r}'_{\text{im}}$ is the reflection of $\mathbf{r}'$ across the image plane. In addition, care must be taken in computing the $\nabla' G(\mathbf{r},\mathbf{r}')\cdot\hat{\mathbf{n}}_i'$ term as well since the normal vector must also be imaged appropriately. The image Green's function produces an electric potential Φ that is an even function about the image plane. This in turn leads to an electrolyte current $\mathbf{J} = -\sigma\nabla\Phi$ whose normal component at the bounding electrolyte-insulator interface is zero.

III. RESULTS

For initial validation, an exterior Neumann problem comprising a one meter sphere with boundary condition [2]:

$$P^f(\Phi) = \frac{\partial \Phi}{\partial n^i} = \Phi + \cos\theta + 3, \quad 0 \le \theta \le \pi, \quad (12)$$

representing a cathodic surface was analyzed. The analytic solution is:

$$\Phi(\mathbf{r}) = -3 - \cos\theta / (3r^2), \quad (13)$$

with $\Phi^\infty = -3$. The discretization in (9) was used and the Newton-Raphson iteration converged in one step. The sphere was discretized with 10th order quadrilateral elements and two meshes of 24 cells and 96 cells were analyzed for various LCN basis orders.

The RMS relative error in the surface potential at the system quadrature points versus basis order is plotted in Fig. 1. The relative error decreases as the basis order increases, but the convergence can stagnate due to the integration of the normal derivative $\nabla' G(\mathbf{r},\mathbf{r}') \cdot \hat{\mathbf{n}}_i'$ in the self-term on curved surfaces [6, 11]. In practice, lower errors can be achieved if a local adaptive integration error tolerance is used for the problematic integrals and a tighter error tolerance is used elsewhere. The scheme used in this paper is to use a relatively tight error tolerance everywhere and then relax the error tolerance on-the-fly and re-integrate only for those integrals that are observed not to converge.

To validate the image plane method, a one meter sphere centered at the origin and floating in an electrolytic half-space of conductivity $\sigma = 1$ S/m for $z < 0$ and $\sigma = 0$ S/m for $z > 0$ was investigated using the boundary condition:

$$P^f(\Phi) = \frac{\partial \Phi}{\partial n^i} = \Phi - \cos(\phi)\sin(\theta) + 3, \quad (14)$$

for $\frac{\pi}{2} \le \theta \le \pi$. The analytic solution is:

$$\Phi = -3 + \cos(\phi)\sin(\theta)/(3r^2), \quad \frac{\pi}{2} \le \theta \le \pi, \quad (15)$$

where again $\Phi^\infty = -3$. The problem was solved in three ways: imaging the hemisphere so that the model is a full sphere in an infinite electrolyte, modeling the hemisphere only using the image Green's function, and boxing the electrolyte with a larger outer hemispherical surface and treating the problem as an interior problem. In the latter case, as depicted in Fig. 2, the modeled surface includes the original hemispherical surface, an outer hemispherical surface, and an annular surface at the electrolyte-air interface that connects the two hemispheres. The $\cos(\phi)\sin(\theta)$ variation in (14) is used since the $\cos(\theta)$ variation in (12) does not produce a potential Φ that is symmetric about the electrolyte-air interface as required.

The surfaces in each of the three models were meshed using 8th-order quadrilateral elements with meshes of various densities and the problem was solved using Newton-Raphson iteration for various basis orders. For the boxed-electrolyte model, the problem was solved for outer hemispheres with radii of 8 m, 16 m, 32 m, and 64 m. To keep the problem size manageable, the outer hemispherical surface used a fixed, coarse discretization. The computed electrostatic surface potential and (1) were used to determine the electrostatic potential at various points in the electrolyte.

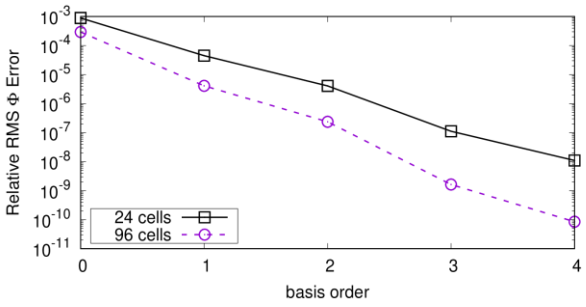

Fig. 1. Relative RMS error between computed and analytic surface potential Φ solutions versus basis order for a one meter sphere meshed with 10th order quadrilateral elements.

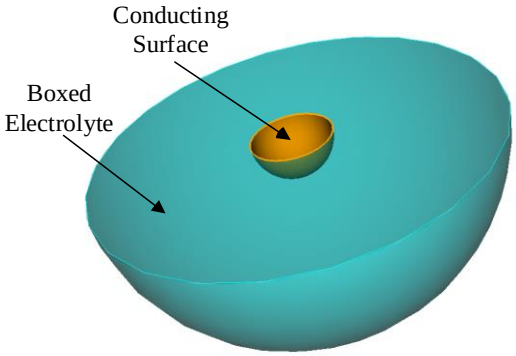

Fig. 2. Hemispherical conducting surface surrounded by a hemispherical-boxed electrolyte.

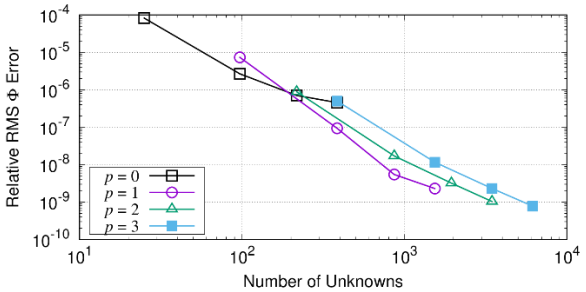

Fig. 3. Error convergence versus number of unknowns for various basis orders p for full sphere model of a hemisphere in an electrolytic half space.

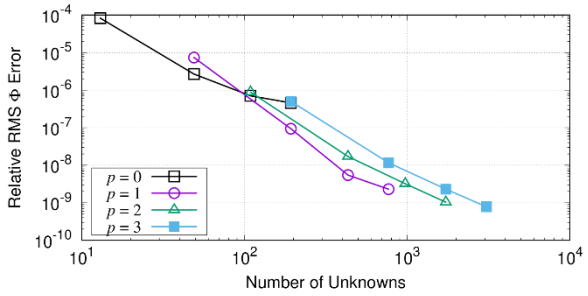

Fig. 4. Error convergence versus number of unknowns for various basis orders p for image plane Green's function model of a hemisphere in an electrolytic half space.

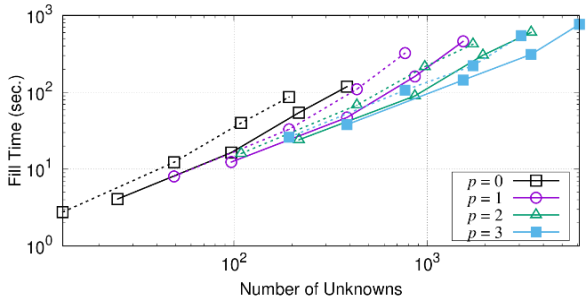

Fig. 5. Fill times versus number of degrees of freedom for full sphere model (solid lines) and half-sphere with image plane Green's function model (dashed lines).

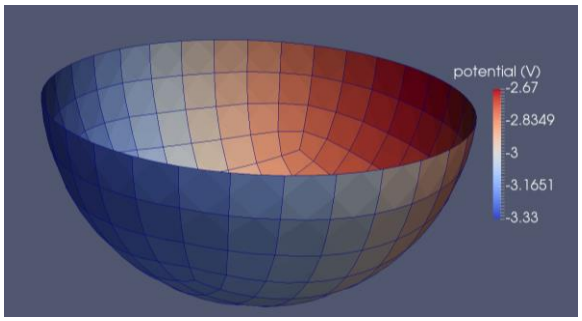

Fig. 6. Surface potential using image plane Green's function model for conducting hemisphere at surface of semi-infinite electrolyte.

The relative RMS error between the computed potential in the electrolyte and the analytic solution is plotted versus number of degrees of freedom in Fig. 3 for the fully imaged sphere and in Fig. 4 for the half-sphere with image plane Green's function. As can be seen from the data, the convergence is the same for both models, but the image plane model requires only half the number of degrees of freedom. Again for each basis order, meshes with an increasing number of elements were analyzed. The matrix fill times versus number of degrees for these two models are plotted in Fig. 5. The use of the image Green's function is clearly more efficient in terms of both the number of degrees of freedom and the computation time. Finally, the surface potential over the hemisphere surface computed using the image plane Green's function model is depicted in Fig. 6 for a mesh of 384 cells and using 2nd order bases.

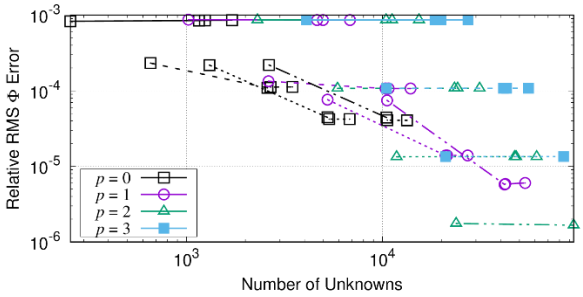

Fig. 7. Error convergence versus number of unknowns for various basis orders p for electrolyte boxed with outer hemispheres of radius a = 8 (solid line), a = 16 m (dashed line), a = 32 m (dotted line), and a = 64 m (dashed-dotted) line.

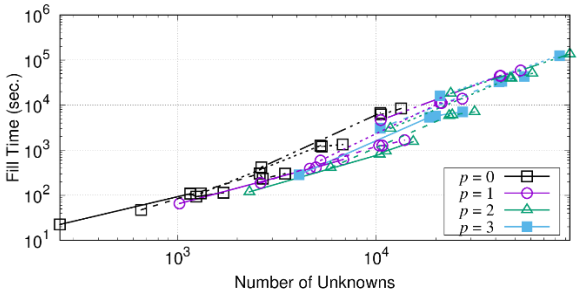

Fig. 8. Fill times versus number of unknowns for various basis orders p for electrolyte boxed with outer hemispheres of radius a = 8 (solid line), a = 16 m (dashed line), a = 32 m (dotted line), and a = 64 m (dashed-dotted) line.

For the last model where the electrolyte is boxed with a finite-radius hemisphere, the error convergence and fill times versus basis order are plotted in Fig. 7 and Fig. 8 respectively. Except for the original conducting hemisphere, the remaining surface mesh is assigned an insulating boundary condition. Hence, the Newton-Raphson iteration can be greatly accelerated using the Schur complement method outlined in II.C. However, in these cases, the matrix fill time dominates the computation time. One observes that the use of a truncated box around the electrolyte severely degrades the error convergence as well as drastically increases the number of unknowns and the computation time. The minimum error is limited by the radius of the outer hemisphere. Hence, the advantages of using image theory are readily apparent.

VI. CONCLUSION

A high-order electrostatic analysis of an impressed current cathodic protection systems was presented. Suitable boundary integral equation formulations were given for both interior and exterior domains, and appropriate constraints to remove any null spaces were discussed. The integral equations were discretized using the locally corrected Nyström method, and problems with nonlinear polarization curves were solved using the Newton-Raphson method. The methods were validated by comparison of computed solutions to analytic solutions for a sphere and hemisphere in an electrolytic half-space and higher-order solution convergence was observed.

ACKNOWLEDGMENT

This work was supported in part by Office of Naval Research Grant N00014-16-1-3066.

REFERENCES

[1] J. M. Chuang, N. G. Zamani, and C. C. Hsuing, "Some computational aspects of BEM simulation of cathodic protection systems," *Applied Mathematical Modelling*, vol. 11, pp. 371-379, October 1987.

[2] N. G. Zamani, J. M. Chuang, and J. F. Porter, "BEM simulation of cathodic protection systems employed in infinite electrolytes," *International Journal for Numerical Methods in Engineering*, vol. 45, pp. 605-620, 1987.

[3] J. F. Yan, S. N. R. Pakalapati, T. V. Nguyen, R. E. White, and R. B. Griffin, "Mathematical modeling of cathodic protection using the boundary element method with a nonlinear polarization curve," *Journal of The Electrochemical Society*, vol. 139, pp. 1932-1936, July 1, 1992.

[4] W. Sun, G. Yuan, and Y. Ren, "Iterative algorithms for impressed cathodic protection systems," *International Journal for Numerical Methods in Engineering*, vol. 49, pp. 751-768, 2000.

[5] R. Pfieffer, "High-order Integral Equation Methods for Quasi-Magnetostatic and Corrosion-Related Field Analysis with Maritime Applications," Ph.D., Electrical & Computer Engineering, University of Kentucky, Lexington, KY, 2018.

[6] J. C. Young, R. Pfeiffer, R. J. Adams, and S. D. Gedney, "Locally corrected Nyström discretization for impressed current cathodic protection systems," presented at the *2018 International Applied Computational Electromagnetics Society Symposium (ACES)*, Denver, CO, 2018.

[7] S. D. Gedney, "On deriving a locally corrected Nyström scheme from a quadrature sampled moment method," *IEEE Transactions on Antennas and Propagation*, vol. 51, pp. 2402-2412, September 2003.

[8] S. D. Gedney and J. C. Young, "The locally corrected Nystrom method for electromagnetics," in *Computational Electromagnetics: Recent Advances and Engineering Applications*, R. Mittra, Ed., New York: Springer, pp. 149-198, 2014.

[9] L. F. Canino, J. J. Ottusch, M. A. Stalzer, J. L. Visher, and S. M. Wandzura, "Numerical solution of the Helmholtz equation in 2D and 3D using a high-order Nyström discretization," *Journal of Computational Physics*, vol. 146, pp. 627-663, 1998.

[10] G. C. Hsiao and W. L. Wendland, *Boundary Integral Equations*. vol. 164, Berlin: Springer-Verlag, 2008.

[11] R. Pfeiffer, J. C. Young, and R. J. Adams, "Numerical characterization of divergence-conforming constrained basis functions for surface integral equations," *IEEE Transactions on Antennas and Propagation*, vol. 65, pp. 1867-1874, 2017.

John C. Young received the B.E.E. degree in Electrical Engineering from Auburn University in 1997, the M.S. degree in Electrical Engineering from Clemson University in 2000, and the Ph.D. degree in Electrical Engineering also from Clemson University in 2002. He received a National Science Foundation Graduate Fellowship in 1998 and served as a Graduate Research Assistant at Clemson University from 1997 to 2002. He is currently an Assistant Professor in the Department of Electrical and Computer Engineering at the University of Kentucky, Lexington, KY. He is a Senior Member of the IEEE and a Member of URSI Commission B, Tau Beta Pi, and Eta Kappa Nu.

Robert Pfeiffer received the B.A. degree in Liberal Arts from Thomas Aquinas College, Santa Paula, CA, USA, in 2012, and the M.S. and Ph.D. degrees in Electrical Engineering from the University of Kentucky, Lexington, KY, USA, in 2015 and 2018, respectively. He studied Electrical Engineering at the Milwaukee School of Engineering in Milwaukee, WI, USA, from 2012 to 2014, and was an Intern with Johnson Controls Inc., Milwaukee, from 2013 to 2014. Since 2014, he has been a Graduate Research Assistant with the University of Kentucky. He is currently with Sandia National Laboratories.

Robert J. Adams received the B.S. degree from Michigan Technological University, Houghton, MI, USA, in 1993, and the M.S. and Ph.D. degrees in Electrical Engineering from Virginia Tech, Blacksburg, VA, USA, in 1995 and 1998, respectively. From 1999 to 2000, he was a Research Assistant Professor with Virginia Tech. He is currently a Professor with the Department of Electrical and Computer Engineering, University of Kentucky, Lexington, KY, USA. His current research interests include applied and computational electromagnetics.

Stephen D. Gedney received the B.Eng.-Honors degree from McGill University, Montreal, P.Q., in 1985, and the M.S. and Ph.D. degrees in Electrical Engineering from the University of Illinois, Urbana-Champaign, IL, in 1987 and 1991, respectively. He is currently the Chair and the Don and Karen White Professor of the Department of Electrical Engineering at the University of Colorado Denver (UCD). Previously he was a Professor of Electrical Engineering at the University of Kentucky from 1991–2014. He worked for the U.S. Army Corps of Engineers, Champaign, IL (’85-’87). He was a visiting Professor at the Jet Propulsion Laboratory, (92’,93’), HRL laboratories (’96-’97) and Alpha Omega Electromagnetics (’04-’05). He received the Tau Beta Pi Outstanding Teacher Award in 1995 and 2013. From 2002–2014, he was the Reese Terry Professor of Electrical and Computer Engineering at the University of Kentucky. He is a past Associate Editor of the IEEE Transactions on Antennas and Propagation (1997–2004), a Member of the IEEE Antennas and Propagation Society ADCOM (2000–2003), and served as the Chair of the IEEE Antennas and Propagation Society Membership Committee (1995–2002). He is a Fellow of the IEEE and Member of Tau Beta Pi.